Published in final edited form as:
Am J Psychiatry. 2012 June 1; 169(6): 589–600. doi:10.1176/appi.ajp.2011.11091447.

Differences in White Matter Fiber Tract Development Present from 6 to 24 Months in Infants with Autism

Jason J. Wolff, Ph.D.[1], **Hongbin Gu, Ph.D.**[1,2], **Guido Gerig, Ph.D.**[1,3], **Jed T. Elison, Ph.D.**[1,4], **Martin Styner, Ph.D.**[1,2], **Sylvain Gouttard, M.S.**[3], **Kelly N. Botteron, M.D.**[5,6], **Stephen R. Dager, M.D.**[7], **Geraldine Dawson, Ph.D.**[2,8], **Annette M. Estes, Ph.D.**[9], **Alan Evans, Ph.D.**[10], **Heather C. Hazlett, Ph.D.**[1,2], **Penelope Kostopoulos, Ph.D.**[10], **Robert C. McKinstry, M.D., Ph.D.**[6], **Sarah J. Paterson, Ph.D.**[11], **Robert T. Schultz, Ph.D.**[11], **Lonnie Zwaigenbaum, M.D.**[12], and **Joe Piven, M.D.**[1,2] **for the IBIS Network***

[1]Carolina Institute for Developmental Disabilities, University of North Carolina, Chapel Hill, NC

[2]Department of Psychiatry, University of North Carolina, Chapel Hill, NC

[3]Scientific Computing and Imaging Institute, University of Utah, Salt Lake City, UT

[4]Division of Humanities and Social Sciences, California Institute of Technology, Pasadena, CA

[5]Department of Psychiatry, Washington University, St. Louis, MO

[6]Department of Radiology, Mallinckrodt Institute of Radiology, Washington University School of Medicine, St. Louis, MO

[7]Department of Radiology, University of Washington, Seattle, WA

[8]Autism Speaks, New York, NY

[9]Department of Speech and Hearing Sciences, University of Washington, Seattle, WA

[10]Montreal Neurological Institute, McGill University, Montreal, QC

[11]Center for Autism Research, Children's Hospital of Philadelphia, and University of Pennsylvania PA

[12]Department of Pediatrics, University of Alberta, Edmonton, AB

Abstract

OBJECTIVE—Evidence from prospective high-risk infant studies suggests that early symptoms of autism usually emerge late in the first- or early in the second-year of life after a period of relatively typical development. This is the first neuroimaging study to prospectively examine white matter fiber tract organization during this interval in infants who develop autism spectrum disorder (ASD) by 24 months.

METHOD—Participants included 92 infant siblings from an ongoing imaging study of autism. All participants had diffusion tensor imaging at 6 months and behavioral assessments at 24 months,

Corresponding author: Jason Wolff, Ph.D., Carolina Institute for Developmental Disabilities, UNC – Chapel Hill, CB# 3366, Chapel Hill, NC 27599, jason.wolff@cidd.unc.edu.

*The IBIS Network. Clinical Sites: University of North Carolina: J. Piven (IBIS Network PI), H.C. Hazlett, C. Chappell; University of Washington: S. Dager, A. Estes, D. Shaw; Washington University: K. Botteron, R. McKinstry, J. Constantino, J. Pruett; Children's Hospital of Philadelphia: R. Schultz, S. Paterson; University of Alberta: L. Zwaigenbaum; Data Coordinating Center: Montreal Neurological Institute: A.C. Evans, D.L. Collins, G.B. Pike, P. Kostopoulos; Samir Das; Image Processing Core: University of Utah: G. Gerig; University of North Carolina: M. Styner; Statistical Analysis Core: University of North Carolina: H. Gu; Genetics Analysis Core: University of North Carolina: P. Sullivan, F. Wright.

Competing interests: All study authors report no financial relationships with commercial interests.

with a majority contributing additional imaging data at either or both 12 and 24 months. At 24 months, 28 infants met criteria for ASD; 64 infants did not. Microstructural properties of white-matter fiber tracts reported to be associated with ASD or related behaviors were characterized by fractional anisotropy (FA) and radial and axial diffusivity.

RESULTS—FA trajectories differed significantly between infants who did versus did not develop ASD for 12 of 15 fiber tracts. Development for most fiber tracts in infants with ASD was characterized by elevated FA at 6 months followed by slower developmental change overtime relative to infants without ASD. Thus, by 24 months of age, lower FA values were evident for those with ASD.

CONCLUSION—These results suggest that the aberrant development of white matter pathways precede the manifestation of autistic symptoms in the first year of life. Longitudinal data are critical to characterizing the dynamic age-related brain and behavior changes underlying this neurodevelopmental disorder.

Autism spectrum disorder (ASD) is a complex neurodevelopmental disorder defined by patterns of impaired social-communication and restricted, repetitive behaviors. ASD represents a significant public health concern, affecting upward of 1 in 110 children with a recurrence rate among at-risk families of nearly 1 in 5 (1, 2). Findings from prospective studies of infant siblings of children with ASD, who are at high familial risk for the disorder, indicate that a number of the defining behavioral features of ASD first emerge around 12 months of age following a period of relatively typical postnatal development (3–4).

Although several studies have now documented the early behavioral course of infants later diagnosed with ASD, there have been no published neuroimaging data on such infants before toddlerhood. Existing neuroimaging studies have provided evidence of significantly enlarged brain volume in two- and three-year olds with ASD using magnetic resonance imaging (MRI) (6–10). These findings are consistent with reports of increased brain weight in postmortem brains of autistic individuals (11), as well as numerous reports associating ASD with a general increase in head circumference (12). Two large retrospective studies suggest that this onset of increased head circumference is likely to occur in the latter part of the first year of life (7, 13). Taken together, findings from high risk infant sibling behavioral studies and studies of brain and head size growth suggest that the latter half of the first year of life is a pivotal time for both brain changes and symptom onset in infants later diagnosed with ASD. The concurrent timing of these phenomena suggests that brain changes during this period may have an important role in the pathogenesis of autistic behavior.

Autism is increasingly considered a disorder characterized in part by aberrant neural circuitry (14, 15). Functional neuroimaging studies have revealed patterns of disrupted functional connectivity in adults (16) and children (17, 18) with ASD. A growing body of work has employed diffusion tensor imaging (DTI) to gauge the microstructural properties of white matter circuitry (19, 20). DTI studies have identified evidence of widespread abnormalities in white matter fiber tract integrity among children and adults with ASD compared to controls (21–25). Results from cross-sectional studies of children and adolescents with ASD (26–27) have revealed both lower fractional anisotropy (FA) and less change associated with age compared to typical controls for a number of fiber tracts. Conversely, others have found increased FA and parallel age associations in young children with ASD compared to controls (28). While the preponderance of existing work suggests altered white matter development in ASD, the extent, direction, and developmental course of these differences remains unclear.

Fundamentally a disorder of development, ASD emerges early in life and is generally associated with life-long disability (29). When development itself is intrinsic to the

phenomenon in question, it becomes necessary to seek answers from developmental trajectories (30–32). This is particularly so in the earliest periods of infancy when dramatic changes in behavior are paralleled by dramatic changes in the brain. White matter pathways, for instance, rapidly develop during the first two years of life, after which change is attenuated (35). To date, however, there are no longitudinal studies of neural circuitry in ASD, and but a few concerning volumetric brain development (8, 33, 34). Although numerous cross-sectional studies of children with ASD posit key neurological changes relevant to the disorder, few employ a true developmental perspective. As Karmiloff-Smith (36) aptly observes, cross-sectional neuroimaging studies of children are not tantamount to neuroimaging studies of *development*.

We present here the first prospective, longitudinal study of early postnatal white matter fiber tract development at 6, 12, and 24 months of age in infants who are at high familial risk for ASD by virtue of having an older sibling with the disorder. In this study, we compare the subset of high risk infants who show evidence of ASD by 24 months of age to those who do not. Given that both groups have a higher familial liability for ASD than the general population, this design allows for inferences not afforded to comparisons of high risk children with ASD to children at low familial risk. The focus of this study is on the development of white matter pathways selected on the basis of reported associations with ASD or core behavioral features of the disorder (21–28).

Methods

Participants

This study includes data from an NIH-funded Autism Center of Excellence (ACE). The parent ACE Network is an ongoing brain imaging study of infants who are at risk for autism. Four clinical data collection sites are associated with the study: University of North Carolina at Chapel Hill, University of Washington in Seattle, Children's Hospital of Philadelphia, and Washington University in St. Louis. All data were coordinated through the Montreal Neurological Institute at McGill University, and data processing performed at the University of North Carolina and the SCI Institute at the University of Utah. The parent study enrolled and assessed 6 month old high-risk (HR) infants who were also seen for follow-up assessments at 12 and 24 months of age. Written informed consent was obtained from the parent or legal guardian of each participant prior to enrollment.

Exclusionary criteria included the following conditions: (1) significant medical conditions known to affect brain development, (2) sensory impairments, (3) low birth weight (<2200g) or prematurity (<36 weeks gestation), (4) evidence of perinatal brain injury secondary to maternal complications or exposure to specific medications or neurotoxins (e.g., alcohol) during gestation, (5) non-English speaking families, (6) evidence for contraindication for MRI (e.g., metal implants), (7) adopted children, and (8) family history of first degree relative with idiopathic intellectual disability, psychosis, schizophrenia, or bipolar disorder.

The present sample included all HR infant siblings with diffusion-weighted MRI scans at 6 months who had completed behavioral assessments at 24 months of age as of June 2011. Symptoms of ASD were measured at 24 months using the Autism Diagnostic Observation Schedule (37) by research-reliable administrators to maximize agreement across sites. HR infants were divided into two groups based on ADOS classifications: HR(−) (below ASD cutoff) and HR(+) (above ASD cutoff). The Mullen Scales of Early Learning (38) was administered at each visit and Early Learning Composite (ELC) scores at 24 months of age used to characterize general developmental level among the sample. Four subjects (2 HR− and 2 HR+) were missing complete Mullen data at 24 months and 12 month Mullen ELCs were substituted. Descriptive and demographic data are presented in Table 1.

Image Acquisition

MRI brain scans were completed at each clinical site on identical 3T Siemens TIM Trio scanners equipped with 12-channel head coils during natural sleep. The DTI sequence was acquired as an ep2d_diff sequence with FoV = 190 mm (6 and 12 months), and FoV = 209 mm (24 months), 75–81 transversal slices, slice thickness = 2 mm isotropic, $2\times2\times2mm^3$ voxel resolution, TR = 12800–13300 ms, TE = 102 ms, variable b-values between 0 and 1000 s/mm^2, 25 gradient directions and scan time of 5–6 minutes. Intra- and inter-site reliabilities were initially established and regularly evaluated via a human traveling phantom study (39).

Image Pre-processing

DWI image data were screened for subject motion and common artifacts related to diffusion sequences using the DTIprep software (40). This tool automatically detects artifacts, corrects for motion and eddy current based deformations, and excludes individual volumetric DWI images with artifacts and generates a full report. Expert raters manually removed DWI scans with clear, residual artifacts. Datasets with less than 18 (70%) gradient DWI images remaining after this quality procedure were excluded from further processing and analysis due to the resulting reduction in signal-to-noise.

DTI Processing Pipeline

The group analysis of DWI data, here processed via diffusion tensor estimates and analysis, employed a recently developed processing pipeline (41). This processing overcomes the major challenge of implementing tract oriented statistics in large study populations, which is finding a consistent spatial parametrization within and between populations. The pipeline includes a computational anatomy approach for nonlinear co-registration of all DTI data to a template reference coordinate frame, a fiber tract oriented process to parameterize tracts to functions of tract length, and mapping of individual tract geometries into common tract coordinates.

Computational Anatomy Mapping

Unbiased atlas building (42) was used to provide a one-to-one mapping between individual subjects' image data and the template atlas, where the atlas reference image is built from the population of image data as the centered image with least deformation distances. The registration proceeds in two steps (41). A first step applies linear, affine registration of the DWI baseline images to a structural weighted T2 atlas using B-spline registration and normalized mutual information (43). This is followed by an unbiased, deformable atlas building procedure (42) that applies large deformation diffeomorphic metric mapping transformations. The procedure relates each individual dataset to the study-specific atlas template space via a nonlinear, invertible transformation. Tensor maps were calculated from each DWI dataset using weighted least squares estimation, and transformed into the atlas space with tensor re-orientation by a finite strain approach (44). The transformed DTI tensor images are averaged using the Riemannian framework (45), resulting in the final 3D average tensor atlas to be used as the reference frame for tractography and tract parameterization. For this study, the longitudinal DWI data of each subject covering the age range of 6 to 24 months were processed with the procedure described above, with all subjects at all ages mapped into the same atlas space.

Fiber Tractography

Seed label maps were created based on methods described in existing tractography atlases (46, 47) and drawn in the combined atlas for regions of interest (ROI) using 3D Slicer (www.slicer.org). A secondary check of ROIs was made using the early childhood DTI atlas

(35). Label maps were created for the following fiber tracts: the genu, body, and splenium of the corpus callosum (CC), fornix, inferior longitudinal fasciculus (ILF), uncinate fasciculus (UF), anterior thalamic radiations (ATR), and the anterior and posterior limbs of the internal capsule (ALIC and PLIC). Label maps were created bilaterally for all tracts with the exception of the CC. Fiber tracts generated in 3D Slicer were processed for spurious or incomplete streamlines using open-source software developed in-house (FiberViewer; http://www.ia.unc.edu/dev/). Fractional anisotropy (FA) values were generated for each fiber tract. FA is an index measuring the degree of anisotropy of local diffusivity, ranging from 0 for isotropic diffusion in fluid to 1 for strongly directional diffusivity in highly structured axonal bundles (18, 19). Axial (AD; λ_1) and radial [RD; $(\lambda_{2,} + \lambda_3)/2$] diffusivity values, which represent diffusion parallel and transverse to axonal directions, were also produced for each fiber tract.

Statistical Analysis

Demographic characteristics were compiled for HR(+) and HR(−) groups at 6, 12 and 24 month time points. Potential group differences were tested for age, sex, and Mullen ELC at each time point using either t-tests (age and Mullen score) or Fisher's exact test (sex).

Longitudinal trajectories of mean FA values for each fiber tract were compared between HR(+) and HR(−) groups using random coefficient linear growth curve models. The random coefficient model is able to fit a group developmental trend while accounting for variability in individual growth trajectories. Among the 92 HR subjects included for the analysis, 14 subjects had 1 visit; 40 had 2, and 38 had 3 visits. The mixed -model framework is able to accommodate different missing patterns and unbalanced designs.

Although white matter is known to develop more rapidly in the first year of life than in the second, a linear model was determined to best fit FA change across time given the limited number of available time points. Separate growth curve models were fit for each fiber tract with age, group, and group X age interaction as fix effects, and age intercept and slope as random effects. All growth curve models included 24 month Mullen ELC scores as a covariate. Following interaction findings between age X group, separate growth slopes were estimated for HR(+) and HR(−) groups. Least square mean FA's were estimated for each group and contrasted at 6, 12, and 24 months to highlight differences at each individual time point. To fully characterize FA results, axial and radial diffusivity were examined in a secondary analysis using the above described growth model. Because of the preliminary nature of the present stage of analysis, family-wise alpha was uncorrected for multiple comparisons.

All analyses were done using SAS software (SAS 9.2, Cary, NC).

Results

There were no differences between HR(−) and HR(+) groups in age or sex ratio at 6, 12, or 24 month scans ($p > .10$), or age at 24 month behavioral assessment. Mullen ELC scores were approximately 12 points lower in the HR(+) group than HR(−) in samples at each time point: 6 months, $t(1, 90) = 2.8$, $p = .007$; 12 months, $t(1, 64) = 2.5$, $p = .01$; and 24 months, $t(1, 47) = 2.1$, $p = .04$. Descriptive and demographic data are presented in Table 1.

Slope parameter estimates with standard error are presented for HR(+) and HR(−) groups for all tracts in Table 2. Both HR(−) and HR(+) groups showed significant increases in FA from 6 to 24 months, but the rate of change for the HR(−) group was significantly greater than that for HR(+) for bilateral limbic (fornix) and association (ILF and uncinate) fiber tracts. Individual and mean group trajectories for these tracts are presented in Figure 1. For corpus

callosum subdivisions (Figure 2), change in FA from 6 to 24 months was significantly different for the body of the CC. For projection tracts (ATR, ALIC, and PLIC), growth trajectories of the left ATR and bilateral ALIC and PLIC were significantly steeper for HR(−) infants (Figure 3).

Follow-up cross-sectional analyses for mean FA are presented in Table 3. Mean FA was significantly higher for HR(+) versus HR(−) at the 6 month time point for the left fornix, $t(89) = 2.1$, $p = .04$; the left ILF, $t(89) = 2.6$, $p = .01$; and left uncinate, $t(89) = 2.2$, $p = .03$. Mean FA for the body of the CC was significantly higher in the HR(+) group at 6 months, $t(89) = 2$, $p = .04$. Mean FA for the right PLIC was significantly higher in the HR(+) group at 6 months, $t(89) = 2.1$, $p = .04$; mean FA for the left ALIC was significantly higher in the HR(−) group at 24 months, $t(89) = -2.1$, $p = .04$. FA for the left ATR was significantly higher in HR(−) at both 12 [$t(89) = -2$, $p = .04$] and 24 [$t(89) = -3$, $p = .003$] months.

Results from secondary analyses of axial and radial diffusivities are presented in Table 4. Linear growth trajectories did not differ significantly for these indices of tract diffusion with the exception of the PLIC, for which RD was significantly higher across the 6 to 24 month interval for the HR(+) group.

Discussion

This study represents the first prospective, longitudinal imaging study of infants at-risk for ASD. The findings reveal a distinct and pervasive course of aberrant white matter fiber tract development in HR infants who go on to develop autistic symptoms. Trajectories of fractional anisotropy (FA) values for 12 of the 15 tracts examined in the present study differed significantly between groups. Most fiber tracts for HR(+) infants were characterized by higher FA at 6 months followed by blunted developmental trajectories such that FA was lower by 24 months. Around 12 months of age, HR groups appear similar across all tracts excepting the ATR, potentially indicating differential timing of development for this specific fiber bundle. Understanding why FA values for multiple fiber tracts are elevated at 6 months but show less change over time may be critical to understanding the development of ASD and shed light on the neural mechanisms underlying its onset.

In agreement with findings from typically developing infants, FA values for HR(−) infants were characterized by rapid change during the 6 to 24 month interval (35). The blunted trajectories seen in the HR(+) group are consistent with the reduced FA and comparative absence of age-related associations observed in older children and adolescents with ASD (24, 26, 27), although these patterns may vary by fiber pathway throughout development (25, 28). The differences in white matter development between HR groups observed in this study are particularly striking considering evidence that individuals with ASD and nonaffected family members of individuals with ASD share a neural phenotype consisting of specific structural and functional brain abnormalities (48, 49). In follow-up analysis, we examined axial and radial diffusivities to elucidate FA results. With a few exceptions, trajectories for these diffusivity measures were not significantly different between groups, suggesting that FA results stem in part from the proportional relationship of AD and RD and not from one measure alone.

The altered trajectories of development seen here ostensibly begin in advance of both the onset of clinical symptoms (3–5) and volumetric changes (6, 8), suggesting that core behavioral features of ASD arise from an altered neurobiological foundation. Instantiated by the present results, the organization of neural networks underlying ASD is characterized by atypical patterns of connectivity that differ across systems and time (14–17) and are not specific to any one brain region or behavioral domain. The relevance of developmental

trajectories to understanding these dynamic processes is undeniable (30–32). Had the present study included only cross-sectional data centered at 12 months, for instance, it might have followed that the ATRs are uniquely relevant to the early development of ASD. The wider view afforded by longitudinal data indicate that the ATRs are but one of many fiber tracts implicated in the disorder, with associations at 12 months the product of differential development.

Both highly experience-dependent and less environmentally mediated processes contribute to functional and structural organization of the brain, and the dynamic interplay of these processes over time yield specialized cortical circuits designed to optimally process complex information (50). For example, differences in structural organization prior to a period of experience-dependent developmental processes related to social-cognition (51–53) may decrease neural plasticity through limitations on environmental input, preventing typical neural specialization (50). These alterations could have a ripple effect through decreasing environmental responsiveness and escalating invariance, thus canalizing a specific neural trajectory resulting in the behavioral phenotype that defines ASD. In typical development, the selective refinement of neural connections via axonal pruning (54), along with constructive processes such as myelination (55), combine to yield efficient signal transmission among brain regions. One or both of these mechanisms may underlie the widespread differences in white matter fiber pathways observed in the current study. Intriguingly, our data is consistent with recent evidence from postmortem stereological research (56) and mouse models of autism (57) suggesting that axonal plasticity may be implicated in the development of ASD.

It is clear that the neurodevelopmental story of ASD neither begins at 6 months of age nor ends at 24. Downward extending neuroimaging to infants prior to 6 months would help clarify the temporal origin of diverging trajectories, while extending to later ages would capture increasingly stable neurobehavioral outcomes. Additional data points would likewise refine the calibration of trajectories beyond linear models. A multimodal approach to neuroimaging could potentially sharpen our understanding of early brain changes in ASD, allowing for the investigation of functional and structural covariance. To better understand the mechanisms which engender and maintain the trajectories evidenced here, subsequent research might also consider the role of genetic and epigenetic variables in the development of structural neural circuitry.

Finally, the presence of significant differences in FA at 6 months raises the exciting possibility of developing imaging biomarkers for risk of ASD in advance of symptom onset. Future work might investigate the potential of predictive models for ASD in early infancy, a process which could include refined imaging techniques or combined bio-behavioral markers. Identifying infants at highest risk for ASD before the full syndrome is manifest offers the possibility of implementing behavioral and other interventions during infancy that could reduce or even prevent the manifestation of the full syndrome (58).

There are several limitations to the present study. The absence of a low-risk contrast group limits interpretation of results outside of a familial background for ASD. Although changes in FA correspond to organizational properties indicative of development (19, 35) as well as histological findings (59), it is an imperfect index of white matter microstructure, and may reflect the effects of axonal packing, crossing fibers, or partial volumes related to noise in DTI data (20, 60). In this study, ASD status was based on ADOS scores at 24 months of age. Follow-up diagnostic assessment at 36–48 months will provide greater assurance of diagnostic outcomes.

This study is the first to identify brain changes related to later ASD as early as 6 months of age. The aberrant development of multiple white matter pathways seen here, along with previously reported brain and behavioral change during infancy (3–9), suggest a period of critical importance to the pathogenesis of ASD. A developmental approach to understanding neural and behavioral changes during this time, sensitive to characterizing longitudinal trajectories, is crucial to understanding the complexities inherent to the neurodevelopmental processes implicated in the emergence of ASD.

Acknowledgments

This work was supported by grants from the National Institutes of Child Health and Development, R01 HDO55741, HD055741-S1, P30 HD03110, and T32 HD40127; Autism Speaks, and the Simons Foundation. Further support was provided by the National Alliance for Medical Image Computing (NA-MIC), funded by the NIH through grant U54 EB005149.

We wish to thank our IBIS children and families for their ongoing participation in this longitudinal study. Thanks also to Varun Puvanesarajah and Eric Maltbie for assisting with tractography, and Rachel G. Smith, Cheryl Dietrich, and Mahshid Farzinfar for the DWI/DTI correction and QC efforts.

References

1. Kogan MD, Blumberg SJ, Schieve LA, Boyle CA, Perrin JM, Ghandour RM, Singh GK, Strickland BB, Trevathan E, van Dyck PC. Prevalence of parent-reported diagnosis of autism spectrum disorder among children in the US, 2007. Pediatrics. 2009; 124:1396–1403.
2. Ozonoff S, Young G, Carter A, Messinger D, Yirmiya N, Zwaigenbaum L, Bryson S, Carver LJ, Constantino JN, Dobkins K, Hutman T, Iverson JM, Landa R, Rogers SJ, Sigman M, Stone WL. Recurrence risk for autism spectrum disorders: a baby siblings research consortium study. Pediatrics. 2011; 128:488–495.
3. Landa R, Garret-Mayer E. Development in infants with autism spectrum disorders: a prospective study. J Child Psychol Psychiatry. 2006; 47:629–638. [PubMed: 16712640]
4. Ozonoff S, Iosi A, Baguio F, Cook IC, Hill MM, Hutman T, Rogers SJ, Rozga A, Sangha S, Sigman MB, Young GS. A prospective study of the emergence of early behavioral signs of autism. J Am Acad Child Adolesc Psychiatry. 2010; 49:256–266. [PubMed: 20410715]
5. Zwaigenbaum L, Bryson S, Rogers T, Roberts W, Brian J, Szatmari P. Behavioral manifestations of autism in the first year of life. Int J Neurosci. 2005; 23:143–152.
6. Courchesne E, Karns C, Davis HR, Ziccardi RA, Carper ZD, Tigue HJ, Chisum P, Moses K, Pierce K, Lord C, Lincoln AJ, Pizzo S, Schreibman L, Haas RH, Akshoomoff NA, Courchesne RY. Unusual brain growth patterns in early life in patients with autistic disorder: an MRI study. Neurology. 2001; 57:245–254. [PubMed: 11468308]
7. Hazlett HC, Poe M, Gerig G, Smith RG, Provenzale J, Ross A, Gilmore J, Piven J. Magnetic resonance imaging and head circumference study of brain size in autism: birth through age 2 years. Arch Gen Psychiatry. 2005; 6:1366–1376. [PubMed: 16330725]
8. Hazlett HC, Poe M, Gerig G, Styner M, Chappell C, Smith RG, Vachet C, Piven J. Early brain overgrowth in autism associated with an increase in cortical surface area before age 2 years. Arch Gen Psychiatry. 2011; 68:467–476. [PubMed: 21536976]
9. Schumann CM, Bloss CS, Barnes CC, Wideman GM, Carper RA, Akshoomoff N, Pierce K, Hagler D, Schork N, Lord C, Courchesne E. Longitudinal magnetic resonance imaging study of cortical development through early childhood in autism. J Neurosci. 2010; 30:4419–4427. [PubMed: 20335478]
10. Sparks BF, Friedman SD, Shaw DW, Aylward EH, Echelard D, Artru AA, Maravilla KR, Giedd JN, Munson J, Dawson G, Dager SR. Brain structural abnormalities in young children with autism spectrum disorder. Neurology. 2002; 59:184–192. [PubMed: 12136055]
11. Bailey A, Luthert P, Dean A, Harding B, Janota I, Montgomery M, Rutter M, Lantos P. A clinicopathological study of autism. Brain. 1998; 121:889–905. [PubMed: 9619192]

12. Lainhart JE, Piven J, Wzorek M, Landa R, Santangelo SL, Coon H, Folstein SE. Macrocephaly in children and adults with autism. J Am Academ Child Adolesc Psychiatry. 1997; 36:282–290.
13. Constantino JN, Majmudar P, Bottini A, Arvin M, Virkud Y, Simons P, Spitznagel E. Infant head growth in male siblings of children with and without autism spectrum disorders. J Neurodev Disord. 2010; 2:39–46. [PubMed: 20651949]
14. Belmonte MK, Allen G, Beckel-Mitchener A, Boulanger LM, Carper RA, Webb SJ. Autism and abnormal development of brain connectivity. J Neurosci. 2004; 24:9228–9231. [PubMed: 15496656]
15. Minshew NJ, Williams DL. The new neurobiology of autism: cortex, connectivity, and neuronal organization. Arch Neurol. 2007; 64:945–950. [PubMed: 17620483]
16. Just MA, Cherkassky VL, Keller TA, Minshew NJ. Cortical activation and synchronization during sentence comprehension in high-functioning autism: evidence of underconnectivity. Brain. 2004; 127:1811–1821. [PubMed: 15215213]
17. Di Martino A, Kelly C, Grzadzinski R, Zuo XN, Mennes M, Mairena MA, Lord C, Castellanos FX, Milham MP. Aberrant striatal functional connectivity in children with autism. Biol Psychiatry. 2011; 69:847–856. [PubMed: 21195388]
18. Dinstein I, Pierce K, Eyler L, Solso S, Malach R, Behrmann M, Courchesne E. Disrupted neural synchronization in toddlers with autism. Neuron. 2011; 70:1218–1225. [PubMed: 21689606]
19. Hüppi PS, Dubois J. Diffusion tensor imaging of brain development. Semin Fetal Neonatal Med. 2006; 11:489–497. [PubMed: 16962837]
20. Mori S, Zhang J. Principles of diffusion tensor imaging and its applications to basic neuroscience research. Neuron. 2006; 51:527–539. [PubMed: 16950152]
21. Alexander AL, Lee JE, Lazar M, Boudos R, DuBray MB, Oakes TR, Miller JN, Lu J, Jeong EK, McMahon WM, Bigler ED, Lainhart JE. Diffusion tensor imaging of the corpus callosum in autism. Neuroimage. 2007; 34:61–73. [PubMed: 17023185]
22. Barnea-Goraly N, Lotspeich LJ, Reiss AL. Similar white matter aberrations in children with autism and their unaffected siblings. Arch Gen Psychiatry. 2010; 67:1052–1060. [PubMed: 20921121]
23. Cheon K, Kim Y, Oh S, Park S, Yoon H, Herrington J, Nair A, Koh Y, Jang D, Kim Y, Leventhal BL, Cho Z, Castellanos FX, Schultz RT. Involvement of the anterior thalamic radiation in boys with high functioning autism spectrum disorders: a diffusion tensor imaging study. Brain Res. 201110.1016/j.brainres.2011.08.020
24. Jou RJ, Jackowski AP, Papademetris X, Rajeevan N, Staib LH, Volkmar FR. Diffusion tensor imaging in autism spectrum disorders: preliminary evidence of abnormal neural connectivity. Aust N Z J Psychiatry. 2011; 45:153–162. [PubMed: 21128874]
25. Keller TA, Kana RK, Just MA. A developmental study of the structural integrity of white matter in autism. Neuroreport. 2007; 18:23–27. [PubMed: 17259855]
26. Cheng Y, Chou KH, Chen IY, Fan YT, Decety J, Lin CP. Atypical development of white matter microstructure in adolescents with autism spectrum disorders. Neuroimage. 2010; 50:873–882. [PubMed: 20074650]
27. Shukla DK, Keehn B, Müller R. Tract-specific analyses of diffusion tensor imaging show widespread white matter compromise in autism spectrum disorder. J Child Psychol Psychiatry. 2011; 52:285–296.
28. Weinstein M, Ben-Sira L, Levy Y, Zachor DA, Ben Itzhak E, Artzi M, Tarrasch R, Eksteine PM, Hendler T, Ben Bashat D. Abnormal white matter integrity in young children with autism. Hum Brain Mapp. 2011; 32:534–543. [PubMed: 21391246]
29. Howlin P, Goode S, Hutton J, Rutter M. Adult outcome for children with autism. J Child Psychol Psychiatry. 2004; 45:212–229. [PubMed: 14982237]
30. Giedd JN, Blumenthal J, Jeffries NO, Castellanos FX, Liu H, Zijdenbos A, Paus T, Evans AC, Rapoport JL. Brain development during childhood and adolescence: a longitudinal MRI study. Nat Neurosci. 1999; 2:861–863. [PubMed: 10491603]
31. Karmiloff-Smith A. Development itself is the key to understanding developmental disorders. Trends Cogn Sci. 1998; 2:389–398. [PubMed: 21227254]

32. Shaw P, Greenstein D, Lerch J, Clasen L, Lenroot R, Gogtay N, Evans A, Rapoport J, Giedd J. Intellectual ability and cortical development in children and adolescents. Nature. 2006; 440:676–679. [PubMed: 16572172]
33. Courchesne E, Campbell K, Solso S. Brain growth across the life span in autism: age-specific changes in anatomical pathology. Brain Res. 2011; 1380:138–145. [PubMed: 20920490]
34. Hardan AY, Libove RA, Keshavan MS, Melhem NM, Minshew NJ. A preliminary longitudinal magnetic resonance imaging study of brain volume and cortical thickness in autism. Biol Psychiatry. 2009; 66:320–326. [PubMed: 19520362]
35. Hermoye L, Saint-Martin C, Cosnard G, Lee S, Kim J, Nassogne MC, Menten R, Clapuyt P, Donohue PK, Hua K, Wakana S, Jiang H, van Zilj PC, Mori S. Pediatric diffusion tensor imaging: normal database and observation of the white matter maturation in early childhood. Neuroimage. 2006; 29:493–504. [PubMed: 16194615]
36. Karmiloff-Smith A. Neuroimaging of the developing brain: taking “developing” seriously. Hum Brain Mapp. 2010; 31:934–941. [PubMed: 20496384]
37. Lord, C.; Rutter, M.; DiLavore, PC.; Risi, S. Autism Diagnostic Observation Schedule. Los Angeles, CA: Western Psychological Services; 2000.
38. Mullen, EM. Mullen Scales of Early Learning: AGS edition. Circle Pines, MN: AGS Publishing; 1995.
39. Gouttard S, Styner M, Prastawa M, Gerig G. Assessment of reliability of multi-site neuroimaging via traveling phantom study. Med Image Comput Assist Interv. 2008; 11(Pt 2):263–270.
40. Liu Z, Wang Y, Gerig G, Gouttard S, Tao R, Fletcher T, Styner MA. Quality control of diffusion weighted images. SPIE Medical Imaging. 2010; 7628:76280J.
41. Goodlett CB, Fletcher PT, Gilmore JH, Gerig G. Group analysis of DTI fiber tract statistics with application to neurodevelopment. Neuroimage. 2009; 45(suppl):133–142.
42. Joshi S, Davis B, Jomier M, Gerig G. Unbiased diffeomorphic atlas construction for computational anatomy. Neuroimage. 2004; 23(suppl 1):151–S160.
43. Rueckert D, Sonoda LI, Hayes C, Hill DLG, Leach MO, Hawkes DJ. Non-rigid registration using free-form deformations: application to breast MR images. IEEE Trans Med Imaging. 1999; 18:712–721. [PubMed: 10534053]
44. Alexander D, Pierpaoli C, Basser PJ, Gee J. Spatial transformations of diffusion tensor magnetic resonance images. IEEE Trans Med Imag. 2001; 20:1131–1140.
45. Fletcher PT, Joshi S. Riemannian geometry for the statistical analysis of diffusion tensor data. Signal Processing. 2007; 87:250–262.
46. Catani M, Thiebaut de Schotten M. A diffusion tensor imaging tractography atlas for virtual in vivo dissections. Cortex. 2008; 44:1105–1132. [PubMed: 18619589]
47. Mori, S.; Wakana, S.; Nagae-Poetscher, LM.; van Zilj, PCM. MRI atlas of human white matter. Amsterdam, Netherlands: Elsevier; 2005.
48. Kaiser MD, Hudac CM, Shultz S, Lee SM, Cheung C, Berken AM, Deen B, Pitskel NB, Sugrue DR, Voos AC, Saulnier CA, Ventola P, Wolf JM, Klin A, Vander Wyk BC, Pelphrey KA. Neural signatures of autism. Proc Natl Acad Sci U S A. 2010; 107:21223–21228. [PubMed: 21078973]
49. Lainhart JE, Bigler ED, Bocian M, Coon H, Dinh E, Dawson G, Deutsch CK, Dunn M, Estes A, Tager-Flusterberg H, Folstein S, Hepburn S, Hyman S, McMahon W, Minshew N, Munson J, Osann K, Ozonoff S, Rodier P, Rogers S, Sigman M, Spence MA, Stodgell CJ, Volkmar F. Head circumference and height in autism: a study by the collaborative program of excellence in autism. Am J Med Genet. 2006; 140:2257–2274. [PubMed: 17022081]
50. Johnson MH. Interactive specialization: a domain-general framework for human functional brain development? Dev Cogn Neurosci. 2011; 1:7–21. [PubMed: 22436416]
51. Blasi A, Mercure E, Lloyd-Fox S, Thomson A, Brammer M, Sauter D, Deeley Q, Barker GJ, Renvall V, Deoni S, Gasston D, Williams SC, Johnson MH, Simmons A, Murphy DG. Early specialization for voice and emotion processing in the infant brain. Curr Biol. 2011; 21:1220–1224. [PubMed: 21723130]
52. Carpenter M, Nagell K, Tomasello M. Social cognition, joint attention, and communicative competence from 9 to 15 months of age. Monogr Soc Res Child Dev. 1998; 63:1–143.

53. Kuhl PK, Tsao FM, Liu HM. Foreign-language experience in infancy: effects of short-term exposure and social interaction on phonetic learning. Proc Natl Acad Sci U S A. 2003; 100:9096–9101. [PubMed: 12861072]

54. Luo L, O'Leary DD. Axon regeneration and degeneration in development and disease. Ann Rev Neurosci. 2005; 28:127–156. [PubMed: 16022592]

55. Wake H, Lee PR, Fields RD. Control of local protein synthesis and initial events of myelination by action potentials. Science. 2011; 333:1647–1651. [PubMed: 21817014]

56. Zikopoulos B, Barbas H. Changes in prefrontal axons may disrupt the network in autism. J Neurosci. 2011; 30:14595–14609. [PubMed: 21048117]

57. Testa-Silva G, Loebel A, Giugliano M, de Kock CP, Mansvelder HD, Meredith RM. Hyperconnectivity and slow synapses during early development of medial prefrontal cortex in a mouse model for mental retardation and autism. Cereb Cortex. 201110.1093/cercor/bhr224

58. Dawson G. Early behavioral intervention, brain plasticity, and the prevention of autism spectrum disorder. Dev Psychopathol. 2008; 20:775–803. [PubMed: 18606031]

59. Concha L, Livy DJ, Beaulieu C, Wheatley BM, Gross DW. In vivo diffusion tensor imaging and histopathology of the fimbria-fornix in temporal lobe epilepsy. J Neurosci. 2010; 30:996–1002. [PubMed: 20089908]

60. Mori S, van Zijl PCM. Fiber tracking: principles and strategies- a technical review. NMR Biomed. 2002; 15:468–480. [PubMed: 12489096]

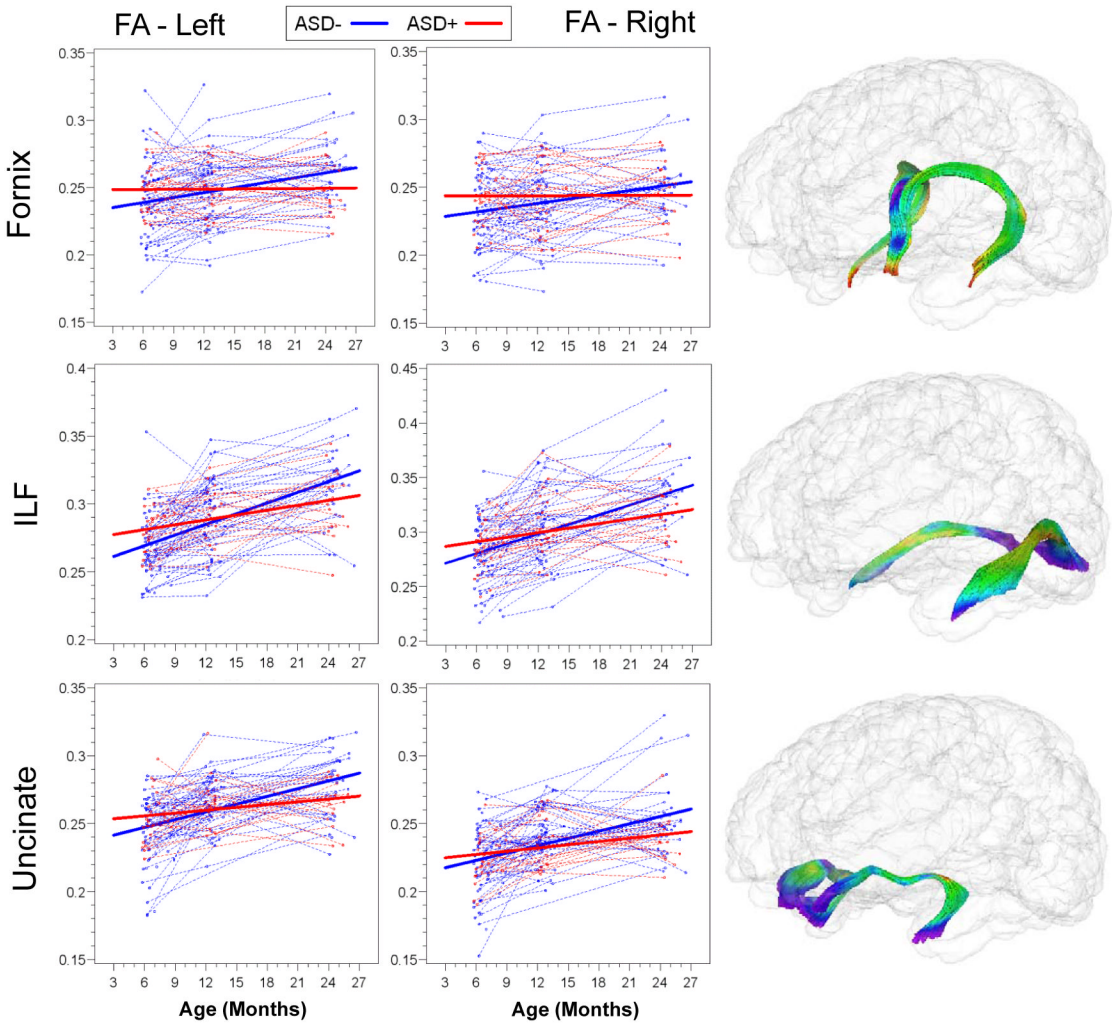

FIGURE 1.
Trajectories of Mean Fractional Anisotropy for High-Risk Groups, Limbic (Fornix) and Association (ILF and Uncinate) Fiber Tracts

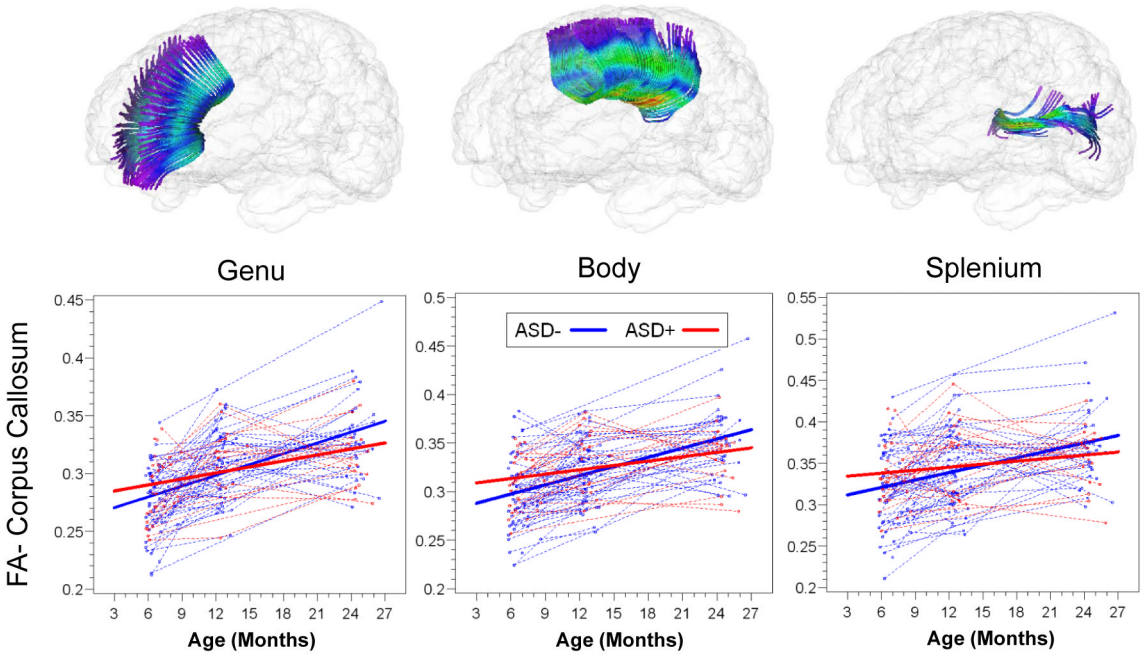

FIGURE 2.
Trajectories of Mean Fractional Anisotropy for High-Risk Groups, Corpus Callosum Subdivisions

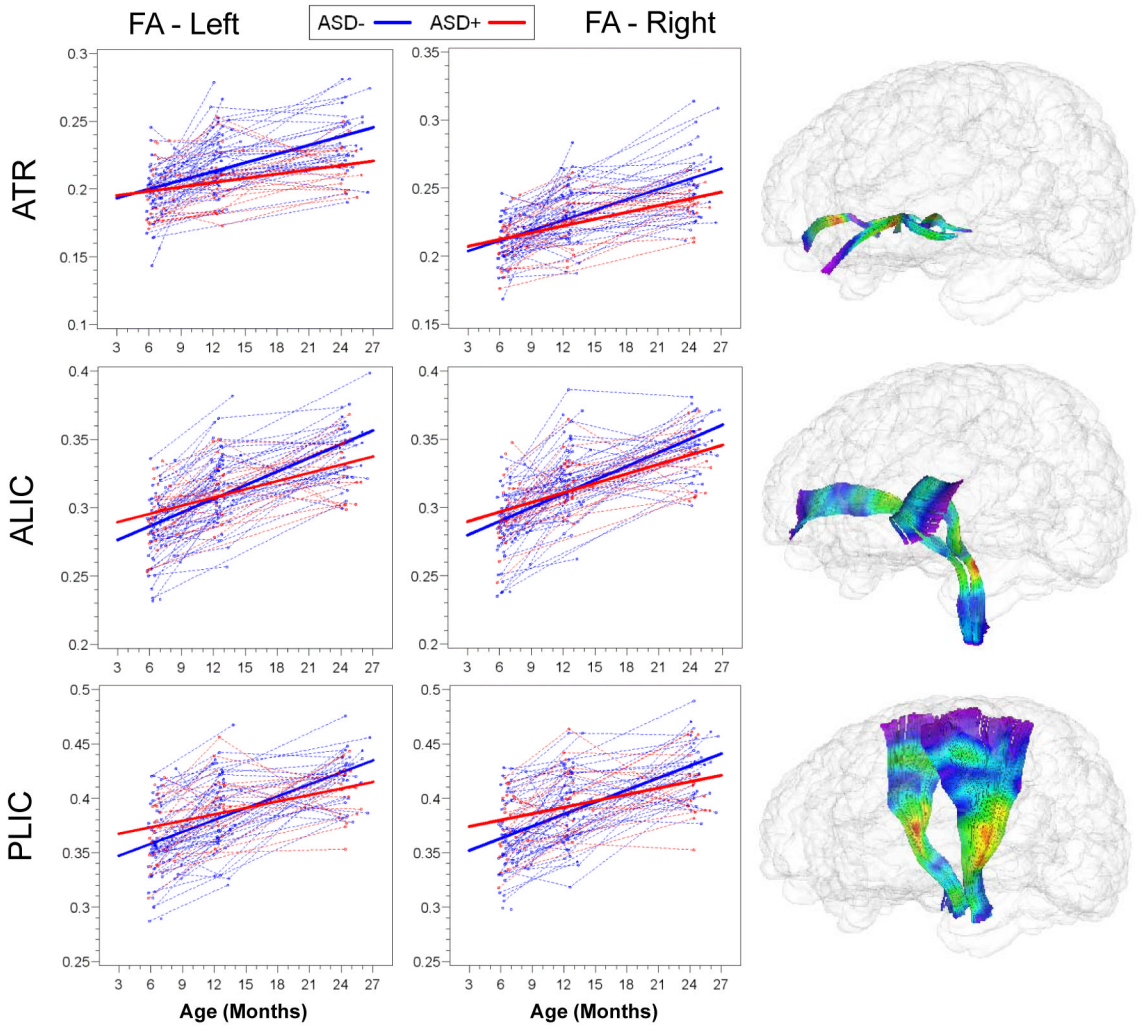

FIGURE 3.
Trajectories of Mean Fractional Anisotropy for High-Risk Groups, Projection Fiber Tracts

TABLE 1

Characteristics of High-Risk Infants with and without Evidence of ASD at 24 Months Age

	N	% Male	Age		Mullen ELC	
			Mean	*SD*	Mean	*SD*
6 months						
HR(+)	28	75	6.8	0.8	90.4[a]	23.7
HR(−)	64	59	6.7	0.8	102.1	15.7
12 months						
HR(+)	17	76	12.7	0.7	89.8[a]	20.3
HR(−)	49	56	12.7	0.6	101.3	14.5
24 months						
HR(+)	17	76	24.5	0.6	86.6[a]	22.0
HR(−)	33	58	24.7	0.8	99.0	18.0

[a]Significant difference, HR(−) > HR(+), $p < .05$

Am J Psychiatry. Author manuscript; available in PMC 2013 June 01.

TABLE 2

Linear Growth Model Estimates for Monthly Mean FA Change Rate ($\times 10^{-3}$)

	HR(+)		HR(−)		Interaction	
Fiber tract	**Slope (SE)**		**Slope (SE)**		***F***	***p***
ALIC, left	2.00	(.36)	3.28	(.25)	8.4	.004
ALIC, right	2.28	(.36)	3.23	(.25)	4.8	.03
ATR, left	1.12	(.33)	2.07	(.23)	5.6	.03
ATR, right	1.74	(.31)	2.38	(.22)	2.8	.1
CC, body	1.56	(.54)	3.10	(.38)	5.4	.02
CC, genu	1.81	(.5)	3.02	(.35)	4.1	.05
CC, splenium	1.33	(.7)	2.94	(.49)	3.6	.06
Fornix, left	0.04	(.36)	1.06	(.25)	5.5	.02
Fornix, right	0.01	(.34)	1.16	(.24)	7.8	.006
ILF, left	1.23	(.36)	2.48	(.25)	8.2	.005
ILF, right	1.32	(.49)	2.91	(.34)	7.2	.009
PLIC, left	1.99	(.45)	3.55	(.31)	8.0	.005
PLIC, right	1.96	(.5)	3.62	(.35)	7.5	.007
Uncinate, left	0.75	(.35)	1.89	(.24)	7.1	.009
Uncinate, right	0.79	(.39)	1.75	(.27)	4.2	.04

Note: ALIC = anterior limb of internal capsule; ATR = anterior thalamic radiation; CC = corpus callosum; ILF = inferior longitudinal fasciculus; PLIC = posterior limb of internal capsule

TABLE 3

Least-Square Mean Estimates for Group Mean FA Difference ($\times 10^{-3}$) at 6, 12, and 24 Months

	6 Months		12 Months		24 Months	
Fiber Tract	**Diff. (SE)**	***p***	**Diff. (SE)**	***p***	**Diff. (SE)**	***p***
ALIC, left	10.1 (5.6)	.07	2.4 (4.5)	.59	−12.9 (6.3)	.04
ALIC, right	7.9 (5.5)	.15	2.2 (4.1)	.59	−9.1 (5.5)	.1
ATR, left	−2.0 (4.4)	.65	−7.7 (3.8)	.05	−19.1 (6.3)	.003
ATR, right	1.1 (3.8)	.76	−2.7 (3.5)	.44	−10.4 (6.2)	.1
CC, body	16.3 (8.0)	.04	7.1 (6.5)	.28	−11.4 (9.6)	.23
CC, genu	10.7 (6.3)	.09	3.4 (5.3)	.53	−11.2 (9.2)	.23
CC, splenium	16.9 (10.4)	.11	7.2 (8.7)	.41	−12.2 (12.7)	.34
Fornix, left	12.3 (5.9)	.04	6.1 (5.2)	.24	−6.1 (7.2)	.4
Fornix, right	9.4 (5.9)	.11	2.5 (4.9)	.62	−11.4 (6.3)	.08
ILF, left	13.2 (5.1)	.01	5.7 (4.4)	.21	−9.4 (4.4)	.18
ILF, right	10.4 (7)	.14	0.9 (6.1)	.89	−18.2 (9.4)	.06
PLIC, left	15.3 (7.8)	.05	6.0 (5.9)	.31	−12.7 (6.7)	.06
PLIC, right	16.2 (7.7)	.04	6.2 (5.9)	.29	−13.7 (7.9)	.08
Uncinate, left	10.6 (4.9)	.03	3.8 (3.8)	.32	−9.8 (5.9)	.1
Uncinate, right	5.3 (5.1)	.3	−0.4 (4)	.92	−11.9 (6.4)	.07

Note:

[a] Difference is in the direction of HR(+) - HR(−)

[b] ALIC = anterior limb of internal capsule; ATR = anterior thalamic radiation; CC = corpus callosum; ILF = inferior longitudinal fasciculus; PLIC = posterior limb of internal capsule

TABLE 4

Linear Growth Model Estimates for Monthly Mean AD and RD Change Rates ($\times 10^{-6}$)

	Axial Diffusivity			Radial Diffusivity		
	HR(+)	HR(−)		HR(+)	HR(−)	
Fiber tract	Slope (SE)	Slope (SE)	*p*	Slope (SE)	Slope (SE)	*p*
ALIC, left	2.3 (1.7)	2.6 (1.2)	.87	−1.2 (1.2)	−3 (0)	.23
ALIC, right	−0.7 (1.3)	1.1 (0)	.25	−3.7 (0)	−3.5 (0)	.89
ATR, left	−6.5 (0)	−5.8 (0)	.46	−6.4 (0)	−7 (0)	.41
ATR, right	−6.2 (0)	−5.2 (0)	.25	−6.6 (0)	−7.1 (0)	.52
CC, body	−10.0 (1.3)	−9.4 (0)	.69	−8.2 (0)	−9.9 (0)	.07
CC, genu	−10.0 (1.2)	−8.1 (0)	.11	−9.1 (0)	−9.1 (0)	.98
CC, splenium	−5.1 (0)	−4.8 (0)	.85	−5.2 (0)	−7.2 (0)	.09
Fornix, left	−7.2 (4)	−10.0 (2.8)	.37	−6 (2.6)	−10 (1.8)	.13
Fornix, right	−4.3 (3.2)	−7.2 (4)	.92	−2.9 (2.6)	−5.4 (1.4)	.33
ILF, left	−10.0 (1.6)	−8.5 (1.1)	.19	−8.2 (0)	−8.8 (0)	.53
ILF, right	−7.7 (1.3)	−6.2 (0)	.36	−6.7 (0)	−7.9 (0)	.18
PLIC, left	−3.6 (0)	−4.4 (0)	.4	−4.5 (0)	−7.4 (0)	.004
PLIC, right	−2.6 (0)	−3.6 (0)	.28	−3.9 (0)	−6.9 (0)	.003
Uncinate, left	−6.5 (0)	−5.9 (0)	.61	−5.4 (0)	−6.6 (0)	.19
Uncinate, right	−6.0 (0)	−5.3 (0)	.44	−5.2 (0)	−6.1 (0)	.29

Note: ALIC = anterior limb of internal capsule; ATR = anterior thalamic radiation; CC = corpus callosum; ILF = inferior longitudinal fasciculus; PLIC = posterior limb of internal capsule